DNA bending by a phantom protein

Juliane K Strauss[1,2], Thazha P Prakash[3], Christopher Roberts[3], Christopher Switzer[3] and L James Maher, III[2]

Background: Despite its stiffness, duplex DNA is extensively bent and folded during packaging and gene expression in biological systems. Modulation of the electrostatic repulsion between phosphates in the DNA backbone may be important in the bending of DNA by proteins. Here, we analyze the shape of DNA molecules that have been modified chemically to mimic the electrostatic consequences of a bound protein.

Results: We have simulated salt bridges between DNA phosphates and cationic amino acid sidechains of a phantom protein by tethering ammonium cations to one face of the DNA helix. Tethered ammonium cations, but not neutral acetylated controls, induce DNA to bend toward its neutralized surface.

Conclusions: The shape of DNA molecules bearing a laterally-asymmetric distribution of tethered cations agrees qualitatively with theoretical predictions and with results previously obtained using neutral phosphate analogs. These data suggest principles that might be applied to the design of artificial DNA-bending proteins.

Addresses: [1]Department of Biochemistry and Molecular Biology, University of Nebraska Medical Center, Omaha, NE 68198, USA, [2]Department of Biochemistry and Molecular Biology, Mayo Foundation, Rochester, MN 55902, USA and [3]Department of Chemistry, University of California at Riverside, Riverside, CA 92521, USA.

Correspondence: L James Maher, III
e-mail: maher@mayo.edu

Introduction

Proteins and polycations can induce DNA to bend and collapse into very compact structures including phage heads [1], toroidal precipitates [2] and the nucleosome itself [3]. DNA compaction in chromatin is equivalent to bending ~84-base-pair (bp) DNA segments into circles. Nevertheless, DNA is an inherently stiff polymer. One measure of DNA stiffness, the j factor, expresses the relative concentration of two DNA sites as a function of the distance between them [4]. The value of j in dilute solution reaches a theoretical maximum of ~100 nM for sites separated by 500–600 bp, but decreases sharply to 1 nM for a 180-bp separation, reflecting the extreme difficulty of bending naked DNA over short distances.

Besides DNA bending induced by protein binding, certain short DNA sequences are known to give rise to electrophoretic and hydrodynamic behavior interpreted as intrinsic static curvature of the double helix. A well-studied example is the five- or six-bp sequence $5'-A_{5-6}$ (only one strand of the duplex is indicated) [5]. According to the prevailing view, this sequence is intrinsically bent by ~18° toward the minor groove in a reference frame shifted by 0.5 bp to the 3' side of the center of the A_{5-6} sequence [6]. Other DNA sequences display intrinsic curvature, though none as dramatic as A_{5-6}. For example, the sequence $5'-G_3C_3$ is intrinsically curved toward the major groove [7,8], whereas some A/T-rich sequences (other than A_{5-6}) are curved by varying degrees toward the minor groove [5].

Nucleoprotein complexes involving bent and looped DNA are important in transcription, replication, and recombination [9]. Two motifs have been observed in protein-induced DNA bending. DNA bending toward a bound protein suggests a role for electrostatic attraction between cationic amino acid sidechains of the protein and the anionic phosphate backbone of DNA. This type of bending occurs when proteins such as *Escherichia coli* CAP [10], or the *Saccharomyces cerevisiae* MATa1 and MATα2 homeodomain proteins [11] are bound to DNA, and in the nucleosome. DNA bending away from a protein occurs in complexes involving intercalation of hydrophobic residues into the minor groove [12]. Proteins that induce this type of bend include HMG box proteins such as SRY and LEF-1, the TATA box-binding protein TBP, the human *ets1* oncogene product ETS1, and the *E. coli* purine repressor protein PurR. A plausible mechanism for DNA bending in this motif is the forced enlargement of the minor groove.

The origin of the free energy needed to distort the structure of DNA in nucleoprotein complexes is of fundamental interest. As originally proposed by Rich and co-workers [13], and investigated theoretically by Manning and co-workers [14], DNA bending toward a bound protein might represent more than a simple electrostatic attraction between the two. These authors argued that asymmetric phosphate neutralization by cationic amino acids could result in unbalanced Coulombic repulsions between phosphates, causing DNA to collapse toward the bound protein (Fig. 1a). Recent

Figure 1
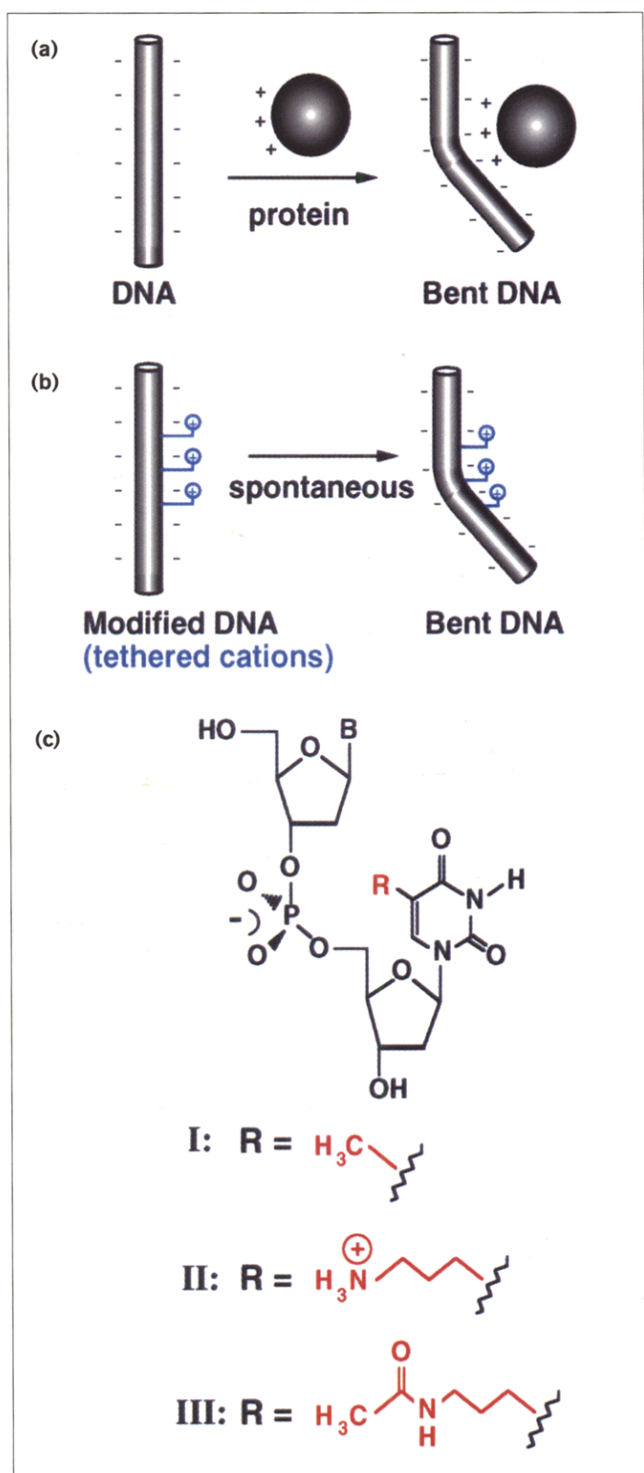
The experimental model and design of these studies. **(a)** DNA bending due to electrostatic interactions between the cationic residues of a DNA-binding protein and the anionic DNA double helix. **(b)** DNA bending by asymmetric incorporation of tethered cations (blue) into the DNA double helix. **(c)** Dinucleotide structure. B denotes an unmodified base. Selected uridine bases are modified at the 5 position by the indicated substitutions (red). I: the normal methyl group in thymine; II: propylamine substitution (cationic at neutral pH); III: acetylated propylamine substitution (neutral).

computational studies suggest that electrostatic effects could also be involved in the mechanism of DNA bending away from a bound protein [15]. In these complexes, Coulombic repulsion between phosphates might be amplified on one face of the DNA helix by replacing the local high dielectric solvent environment with a low dielectric binding protein.

We are studying the prediction that asymmetric phosphate neutralization should induce DNA to bend toward the neutralized face of the double helix. Phosphate neutralization was accomplished in previous experiments by site-specific substitution of neutral methylphosphonates [16]. Neutralization of six phosphates along the DNA minor groove in a G/C-rich sequence induced a ~20° bend in the predicted direction. Although control experiments suggested that this effect was predominantly electrostatic, we have sought here and in a previous study [8] to confirm our conclusions using other salt bridge analogs.

Results and discussion
Strategy
We reasoned that covalent tethering of ammonium ions to one face of the DNA double helix might provide a novel method to simulate asymmetric phosphate neutralization caused by cationic amino acids of a bound protein (Fig. 1b). For this purpose, primary amines (positively charged at neutral pH) were attached via propyl tethers to the 5 position of deoxyuridine residues in synthetic oligonucleotides (Fig. 1c; [17]). This design amounts to appending a small number of lysine analogs near the phosphate backbone on one face of the double helix. As controls, neutral acetylated derivatives of these tethered amines were also analyzed (Fig. 1c).

Electrophoretic detection of DNA bending
We measured DNA curvature by electrophoretic methods. The mobility of a DNA molecule through a native polyacrylamide gel is dependent on both molecular weight and shape [6]. DNA curvature (reduced average end-to-end distance) is manifested as reduced electrophoretic mobility. The intrinsic curvature of A_{5-6} tracts has provided a useful reference, allowing formulation of an empirical relationship between the extent of DNA bending and the degree of electrophoretic retardation [18]. We then used the phasing method to measure the shape of DNA molecules bearing tethered cations. This method places an uncharacterized site of helix deformation (in this case a $5'\text{-}A_3GT_3$ sequence with or without tethered cations) at different positions relative to a reference element of curvature (an A_5 tract) whose magnitude and direction are well characterized. Synthetic DNA duplexes are ligated to amplify shape effects in the resulting polymers. In phasing analysis, the net curvature of the DNA duplex reaches extremes as the deformations are phased, so as to affect either the same DNA face (*cis*

configuration) or opposite DNA faces (*trans* configuration). Phasing analysis allows estimation of both the magnitude and direction of the uncharacterized shape.

Experimental design

Synthetic DNA duplexes (21 bp) forming two helical turns of DNA are shown in Figure 2. These molecules were then ligated enzymatically in a unidirectional orientation [16]. The helical repeat was measured and found to be ~10.5 bp per helical turn in all cases [19]. Each 21-bp duplex contained a single A_5 tract. Duplexes **1–3** contained an unmodified 5'-A_3GT_3 sequence at different distances from the A_5 tract. In duplex **1** the locus of curvature of the A_5 tract is separated from the center of the 5'-A_3GT_3 sequence by 10.5 bp (*cis* configuration). The separations in duplexes **2** and **3** are 8.5 bp (orthogonal) and 6.5 bp (*trans*), respectively. Duplex **4** is a standard containing an A_6 tract but lacking the 5'-A_3GT_3 sequence. Duplexes **5–7** each contain six propylamine modifications (Fig. 2). This substitution pattern places the tethered cations near phosphates along opposite sides of one minor groove (Fig. 3). Phasing of the tethered cations relative to the A_5 tract is as described above for duplexes **1–3**. Duplexes **8–10** are identical to duplexes **5–7**, except that the appended amines are neutralized by acetylation (Fig. 2).

Molecular models depicting the arrangement of tethered cations and bending elements in key DNA duplexes are shown in Figure 3.

Qualitative data

The results of a phasing experiment are shown in Figure 4. The intrinsic shape of the unmodified 5'-A_3GT_3 sequence was first determined by changing its phasing relative to an A_5 tract. The electrophoretic mobility of ligated duplexes lacking the 5'-A_3GT_3 sequence show the anticipated mobility retardation (Fig. 4, e.g., 168-bp species in lane 9 (●) migrates more slowly than 200-bp species in the reference ladder in lane 8). Lanes 2, 4 and 7 demonstrate that changes in the spacing between the A_5 tract and the unmodified 5'-A_3GT_3 sequence resulted in different gel mobilities. The greatest retardation occurred when the minor groove of the unmodified 5'-A_3GT_3 sequence was centered on the same DNA face as the A_5 tract (*cis* configuration, Fig. 4, lane 2). This qualitative result demonstrates that the 5'-A_3GT_3 sequence is intrinsically curved toward the minor groove. Lanes 12, 14 and 17 of Figure 4 demonstrate mobility alterations as a function of the phasing between the A_5 tract and the propylamine-modified 5'-A_3GU_3 sequence. The enhanced mobility difference between *cis* and *trans* configurations indicates that tethered cations induce additional DNA bending toward the minor groove (compare Fig. 4, lanes 12, 14, 17 with lanes 2, 4 and 7). Finally, lanes 19, 22 and 24 of Figure 4 demonstrate that changing the spacing between the A_5 tract and the 5'-A_3GU_3 sequence bearing acetylated

Figure 2
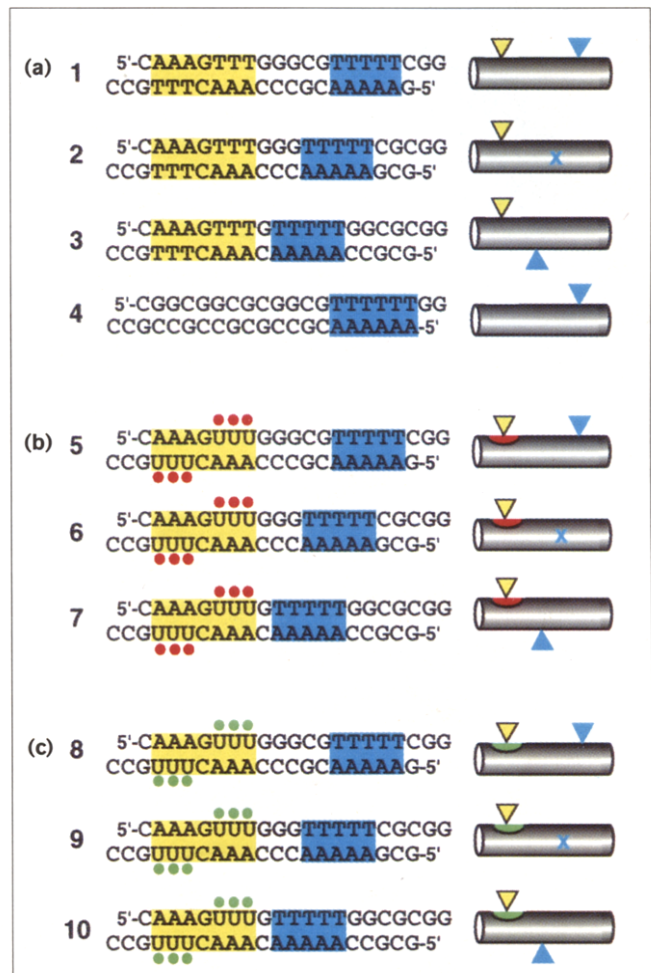
The synthetic oligonucleotides used in these studies. **(a)** Unmodified duplexes **1–3** contain the 5'-A_3GT_3 sequence (yellow) at different distances from an A_5 tract (blue). In duplex **1** the minor groove at the center of the 5'-A_3GT_3 sequence is on the same helical face as the curvature due to the A_5 tract (*cis* configuration). In duplexes **2** and **3** these elements are separated by ~70° (orthogonal configuration) and ~140° (*trans* configuration), respectively. Duplex **4** provides a standard lacking the 5'-A_3GT_3 element. Cylinders at right depict elements of curvature found in these molecules. The concave DNA face caused by intrinsic curvature of an A_5 tract toward the minor groove is indicated by a blue arrowhead (or by a blue 'X' when directed into the plane of the figure). The concave DNA face caused by intrinsic curvature of the unmodified 5'-A_3GT_3 sequence is indicated by a yellow arrowhead. **(b)** Duplexes **5–7** contain the modified 5'-A_3GU_3 sequence (tethered ammonium cations indicated by red circles above uracil residues at left and by red ovals at right) phased with A_5 tracts as described above for duplexes **1–3**. The concave DNA face caused by induced bending occurs at the red oval. **(c)** Duplexes **8–10** are similar to duplexes **5–7**, but contain acetylated (uncharged) modifications. Green circles (left) and green ovals (right) indicate acetylated propylamines.

propylamines results in gel mobilities comparable to those seen for the unmodified 5'-A_3GT_3 sequence.

Together these qualitative observations show that the 5'-A_3GT_3 sequence is intrinsically curved toward the

Figure 3
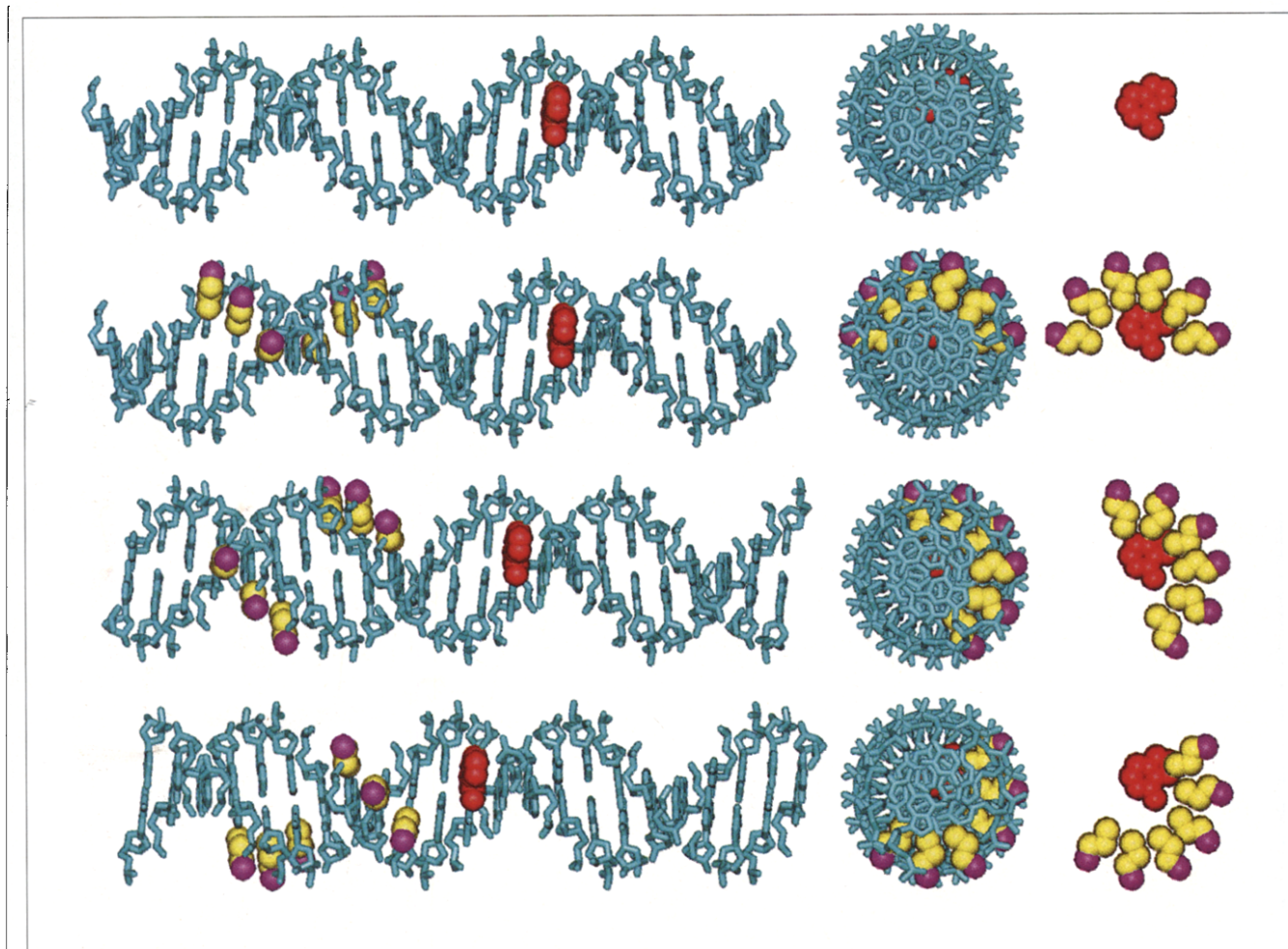
Molecular models of DNA duplexes **1** (unmodified), **5** (*cis*), **6** (orthogonal), and **7** (*trans*). Atoms comprising the 3' adenine of each A$_5$ tract are rendered as red spheres. Atoms comprising the propyl tethers to U residues are shown in yellow, with ammonium ions in magenta. Propyl tethers are depicted in fully extended conformations. For clarity, the disposition of tethered ions is shown at right after removal of DNA atoms. DNA molecules are depicted with flush termini and a helical repeat parameter of 10.5 bp per turn using SYBYL (Tripos). In the case of side views (left), the duplexes are oriented such that intrinsic curvature at the A$_5$ tract would result in the right end of each molecule being curved upward by 18° in the plane of the figure.

minor groove, that tethering six cations on one face of the double helix causes additional DNA bending, as predicted, and that induced bending is not observed when the appended amines are acetylated, suggesting that the effect is electrostatic.

Quantitation of DNA bend angles

Quantitative estimates of the extent of intrinsic or induced bending were deduced from plots of the electrophoretic data (Fig. 5). DNA shape information is depicted graphically by plotting R_L (the ratio of apparent DNA length to actual DNA length) versus the actual length of the ligated duplexes (Fig. 5, panels a–c). The data were then transformed (Fig. 5, panels d–f) to allow fitting to a linear function relating gel anomaly to the relative curvature for each phasing [16,18]. Estimates for net curvature (A$_{5-6}$ tract equivalents per helical turn) were obtained for each phasing. Data were then combined using a phasing function to generate quantitative estimates for the magnitude of the intrinsic or induced bend (Fig. 5g). The results appear in Table 1.

These quantitative data demonstrate that the 5'-A$_3$GT$_3$ sequence is intrinsically curved by ~9° toward the minor groove. When supplemented with six tethered cations, bending toward the minor groove is enhanced to ~17°, suggesting that the appended positive charges induce ~8° of bending. Acetylation of the tethered amines results in a DNA shape indistinguishable from the unmodified duplex, supporting the view that the ammonium cations, rather than the tethers, are responsible for DNA bending.
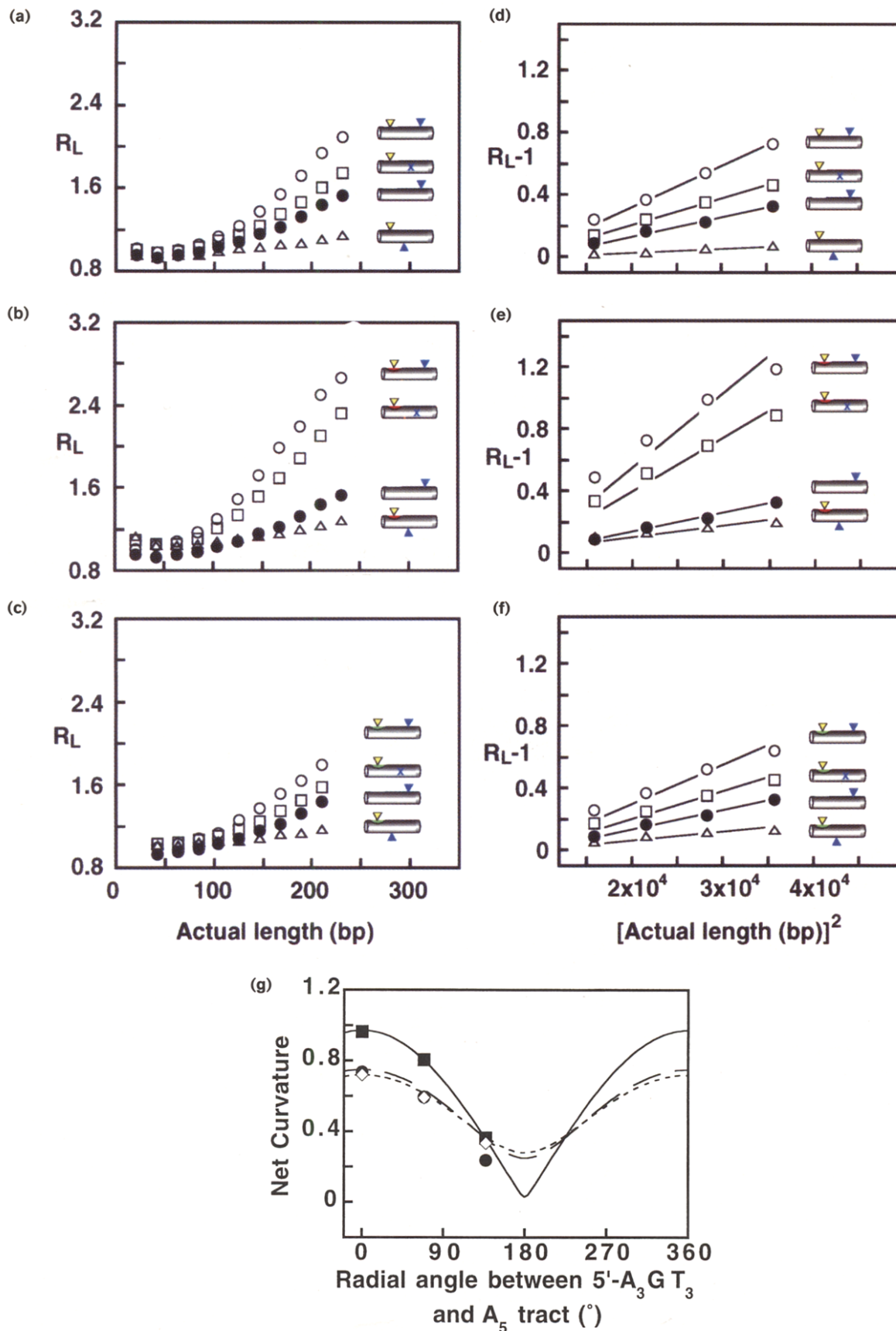
Figure 4

Electrophoretic assay of DNA shape indicates that tethered cations induce DNA bending. Radiolabeled 21-bp DNA duplexes **1–10** were ligated and analyzed by electrophoresis through 5 % nondenaturing polyacrylamide gels as previously described [16]. Band assignments were made with reference to unligated 21-bp duplexes in lanes 1, 5, 6, 10, 11, 15, 16, 20, 21 and 25. Unmodified duplexes appear in lanes 2, 4, 7 and 9. Duplexes modified by tethered ammonium cations appear in lanes 12, 14 and 17. Duplexes modified by tethered acetylated amines appear in lanes 19, 22 and 24. Reference lanes (8, 13, 18 and 23) contain a 100-bp duplex DNA ladder (sizes indicated in lanes 15–16). The 168-bp DNA species for each ligated sample is indicated (●). Color assignments in the DNA symbols are as described in the legend to Figure 2.

Comparison with previous results

The ~8° of bending induced by tethered cations in these experiments is smaller than the ~20° bend induced when a similar pattern of phosphates were completely neutralized by methylphosphonate substitution [16]. This result, however, is greater than the ~4° bend induced in a different DNA sequence by ammonium ions on longer hexyl tethers [8]. Unlike methylphosphonate analogs, flexible tethers presumably allow some diffusion of appended cations over the DNA face [20]. Diffusion of these tethered cations may actually be greater than for cationic amino acid sidechains in DNA–protein complexes, where specific salt bridges to phosphates can be stabilized by networks of other contacts. It is thus tempting to speculate that the bending hierarchy methylphosphonate > propylamine > hexylamine reflects the decreasing extent of phosphate neutralization in this series.

On the other hand, comparative interpretation of bending data are complicated by theoretical [21] and experimentally-observed [22] propensities of different DNA sequences to bend toward either the major or minor groove. Previous experiments with methylphosphonate analogs involved an intrinsically straight, G/C-rich target sequence [16]. In a different study, DNA bending by hexylammonium ions was examined using modified C residues in a G/C-rich sequence context that intrinsically curved toward the major groove [8]. Here, the target sequence for modified T residues was A/T-rich and intrinsically curved toward the minor groove. Additional bending studies will be required to clarify the role of DNA-sequence context.

Significance

Asymmetric tethering of cations to DNA reinforces the conclusion that DNA spontaneously bends when

Figure 5 (facing page)

Tethered cations induce DNA bending. **(a–c)** Graphic depiction of electrophoretic data. Apparent lengths of unmodified DNA duplexes were calculated relative to mobilities of the 100-bp duplex DNA ladder. The ratio of apparent length to actual length, R_L, is a measure of DNA curvature. **(a)** Data demonstrating intrinsic curvature of the 5'-A_3GT_3 element in duplexes **1–3** as compared to duplex **4**. **(b)** Induced DNA bending in modified duplexes **5–7** bearing tethered ammonium cations. **(c)** Absence of induced DNA bending in modified duplexes **8–10** bearing tethered acetylated amines. **(d–f)** Estimation of relative DNA curvature (A_5 tract equivalents per helical turn). Relative DNA curvature estimates were obtained as previously described [16,18]. Standard deviations (2–4 experimental repetitions) were less than 11 % in all cases. The behavior of duplex **4** was used

as a standard (relative curvature set at 0.5 A_5 tract equivalents per helical turn). **(d)** Unmodified duplexes **1–4**. **(e)** Duplexes **5–7** containing tethered ammonium cations. **(f)** Duplexes **8–10** containing tethered acetylated amines. **(g)** Interpretation of phasing data. Plot depicts estimates of the magnitude of net curvature (A_5 tract equivalents per helical turn) as a function of the radial angle between the A_5 tract and the locus of bending under study. Net curvature combines intrinsic curvature due to the A_5 tract and either the intrinsic curvature of the 5'-A_3GT_3 sequence (for unmodified duplexes (●)), or bending induced at the 5'-A_3GU_3 sequence (for tethered ammonium cations (■), or tethered acetylated amines (◇)). Color assignments in the DNA symbols are as described in the legend to Figure 2.

asymmetrically neutralized, and provides a new approach to studying the role of electrostatics in DNA structure. This latent source of DNA-bending energy has been largely unappreciated and may significantly stabilize bent DNA in nucleoprotein complexes such as the nucleosome. Our phantom protein approach offers a unique biochemical strategy for isolating and measuring the electrostatic consequences of protein–DNA interactions by deleting the many additional sources of DNA-bending energy that may accompany protein binding. Our results, obtained using tethered ammonium ions, suggest that previous observations of DNA bending induced by site-specific methylphosphonate substitution indeed reflected electrostatic phenomena. Moreover, the tethered-cation approach has allowed synthesis of control molecules in which the tethered cations are neutralized by acetylation. The fundamental role of electrostatic effects in our observations is confirmed by the inability of these neutralized analogs to induce DNA bending.

High resolution structures of a variety of DNA sequences show that they are bent in complexes with protein. How much of this DNA bending can be generated in the absence of protein simply by chemically neutralizing phosphates that are contacted by cationic amino acid sidechains in the bent complexes? Targets for such analyses could include the *E. coli* CAP-binding

Table 1

Intrinsic and induced DNA curvature.

Duplex	Bending at 5'-A_3GT_3
Unmodified	9 ± 0.4 (4)
Tethered ammonium cations	17 ± 1.4 (4)
Tethered acetylated amines	8 ± 0.7 (2)

DNA-bending estimates (°) based on best fits to phasing equations. Indicated bend angles are toward the minor groove. The average value is given ± standard deviation, based on the number of experiments indicated in parentheses.

sequence, and segments of DNA known to be easily packaged into nucleosomes. Similar phenomena may be important in ribonucleoprotein structures.

Finally, if asymmetric phosphate neutralization is a realistic source of DNA-bending energy, it should be possible to use this principle in the design of novel DNA-bending proteins and other ligands. For example, combining a sequence-specific DNA-recognition motif with an adjacent cationic protein surface should amplify DNA collapse toward the DNA–protein interface in the resulting complex.

Materials and methods

Oligonucleotides

Protected deoxyuridine phosphoramidite monomers containing tethered cations attached via propyl tethers to the 5 position were synthesized and incorporated into oligodeoxyribonucleotides as previously described [17]. Oligomers were purified by denaturing polyacrylamide gel electrophoresis, eluted from the gel, desalted using C_{18} reverse phase cartridges, and characterized by laser desorption mass spectroscopy [23]. Oligonucleotides were radiolabeled by phosphorylation with polynucleotide kinase, annealed, and ligated into molecular ladders as previously described [19].

Electrophoresis

Samples were analyzed on 5 % polyacrylamide gels (29:1 acrylamide:bisacrylamide ratio; 15.8 cm x 22.8 cm x 0.75 mm). Casting and running buffers were 90 mM TBE unless otherwise noted. Electrophoresis was performed at room temperature (11 V cm^{-1}) until the bromophenol blue marker reached 18 cm from the base of the wells. Gels were dried and imaged by storage phosphor technology. The helical repeat parameters for unmodified and modified DNA duplexes were determined by comparing mobilities of molecular ladders resulting from ligation of duplexes of lengths 20, 21, or 22 bp. In all cases, duplexes of length 21 bp maximized electrophoretic retardation, demonstrating that A_5 tracts were most nearly in phase when a helical repeat of 10.5 bp per turn was assumed.

Quantitation of DNA bending

The distance migrated by duplex DNA standards of known length was measured and fit by a least-squares method to an exponential function. The apparent length of DNA in each gel band was then estimated using the derived function and the distance migrated. An equation of the form:

$$R_L - 1 = A \text{ (relative curvature)} \tag{1}$$

was fit by a least-squares method to data for duplexes containing one A_5 tract per 21 bp (relative curvature = 0.5 A_5 tract equivalents per helical turn) and no neutral phosphates. R_L data for 100 bp < duplex length < 170 bp were used for the analysis. This procedure estimates the value of the constant, A, for each gel [18]. The resulting equation was then used to obtain estimates for unknown relative curvature values for duplexes containing both A_5 tracts and neutralized phosphates. This approach is most accurate for DNA molecules with $R_L > 1.2$. Estimates for the magnitude of the electrostatic bend, b, were calculated by obtaining the least-squares fit of the phasing equation (derived from the trigonometric Law of Cosines)

$$c = \sqrt{a^2 + b^2 - 2ab\cos(180 - \theta)} \qquad (2)$$

to plots of the net curvature versus radial angle, θ. Constant a is the magnitude of the curvature due to the A_5 tract (0.5 A_5 tract equivalents per helical turn). Dependent variable c is the measured value of the net curvature (same units), and b is the unknown magnitude of the electrostatic bend (same units). Estimates of net curvature in degrees were obtained using a value of 18° for the deflection of the DNA helix axis by a single A_5 tract [18,24].

Acknowledgements

References
1. Earnshaw, W.C. & Casjens, S.R. (1980). DNA packaging by the double-stranded DNA bacteriophages. *Cell* **21**, 319–331.
2. Chattoraj, O.K., Gosule, L.C. & Schellman, J.A. (1978). DNA condensation with polyamines. II. Electron microscopic studies. *J. Mol. Biol.* **121**, 327–337.
3. Arents, G. & Moudrianakis, E.N. (1993). Topography of the histone octamer surface: repeating structural motifs utilized in the docking of nucleosomal DNA. *Proc. Natl. Acad. Sci. USA* **90**, 10489–10493.
4. Bellomy, G.R., Mossing, M.C. & Record, M.T. (1988). Physical properties of DNA *in vivo* as probed by the length dependence of the lac operator looping process. *Biochemistry* **27**, 3900–3906.
5. Koo, H.-S., Wu, H.-M. & Crothers, D.M. (1986). DNA bending at adenine•thymine tracts. *Nature* **320**, 501–506.
6. Crothers, D.M. & Drak, J. (1992). Global features of DNA structure by comparative gel electrophoresis. *Meth. Enzymol.* **212**, 46–71.
7. Brukner, I., Susic, S., Dlakic, M., Savic, A. & Pongor, S. (1994). Physiological concentration of magnesium ions induces a strong macroscopic curvature in GGGCCC-containing DNA. *J. Mol. Biol.* **236**, 26–32.
8. Strauss, J.K., Roberts, C., Nelson, M.G., Switzer, C. & Maher, L.J. (1996). DNA bending by hexamethylene tethered ammonium ions. *Proc. Natl. Acad. Sci. USA*, in press.
9. Adhya, S. (1989). Multipartite genetic control elements: communication by DNA loop. *Annu. Rev. Genet.* **23**, 227–250.
10. Schultz, S.C., Shields, G.C. & Steitz, T.A. (1991). Crystal structure of a CAP–DNA complex: The DNA is bent by 90°. *Science* **253**, 1001–1007.
11. Li, T., Mead, J., Wolberger, C. & Vershon, A.K. (1995). Structure of the MATa1 and MATα2 homeodomain heterodimer bound to DNA. *Science* **270**, 262–269.
12. Werner, M.H., Gronenborn, A.M. & Clore, G.M. (1996). Intercalation, DNA kinking, and the control of transcription. *Science* **271**, 778–784.
13. Rich, A. (1978). Localized positive charges can bend double helical nucleic acid. *Fed. Eur. Biochem. Soc.* **51**, 71–81.
14. Manning, G., Ebralidse, K.K., Mirzabekov, A.D. & Rich, A. (1989). An estimate of the extent of folding of nucleosomal DNA by laterally asymmetric neutralization of phosphate groups. *J. Biomol. Struct. Dyn.* **6**, 877–889.
15. Elcock, A.H. & McCammon, J.A. (1996). The low dielectric interior of proteins is sufficient to cause major structural changes in DNA on association. *J. Am. Chem. Soc.* **118**, 3787–3788.
16. Strauss, J.K. & Maher, L.J. (1994). DNA bending by asymmetric phosphate neutralization. *Science* **266**, 1829–1834.
17. Hashimoto, H., Nelson, M.G. & Switzer, C. (1993). Zwitterionic DNA. *J. Am. Chem. Soc.* **115**, 7128–7134.
18. Koo, H.-S. & Crothers, D.M. (1988). Calibration of DNA curvature and a unified description of sequence-directed bending. *Proc. Natl. Acad. Sci. USA* **85**, 1763–1767.
19. Rice, J.A. & Crothers, D.M. (1989). DNA bending by the bulge defect. *Biochemistry* **28**, 4512–4516.
20. Liang, G., Encell, L., Nelson, M.G., Switzer, C., Shuker, D.E. & Gold, B. (1995). Role of electrostatics in the sequence-selective reaction of charged alkylating agents with DNA. *J. Am. Chem. Soc.* **117**, 10135–10136.
21. Olson, W.K., Marky, N.L., Jernigan, R.L. & Zhurkin, V.B. (1993). Influence of fluctuations on DNA curvature – a comparison of flexible and static wedge models of intrinsically bent DNA. *J. Mol. Biol.* **232**, 530–554.
22. Brukner, I., Sanchez, R., Suck, D. & Pongor, S. (1995). Sequence-dependent bending propensity of DNA as revealed by DNase I: parameters for trinucleotides. *EMBO J.* **14**, 1812–1818.
23. Pieles, U., Zurcher, W., Schar, M. & Moser, H.E. (1993). Matrix-assisted laser desorption ionization time-of-flight mass spectrometry: a powerful tool for the mass and sequence analysis of natural and modified oligonucleotides. *Nucleic Acids Res.* **21**, 3191–3196.
24. Koo, H.-S., Drak, J., Rice, J.A. & Crothers, D.M. (1990). Determination of the extent of DNA bending by an adenine–thymine tract. *Biochemistry* **29**, 4227–4234.